SUPPORTING INFORMATION

Title:

Tests of species-specific models reveal the importance of drought in postglacial range shifts of a Mediterranean-climate tree: insights from iDDC modelling and ABC model selection

Authors:

Jordan B. Bemmels[1,3], Pascal O. Title[1], Joaquín Ortego[2], L. Lacey Knowles[1]

Author affiliations:

[1] Department of Ecology and Evolutionary Biology, 830 N. University Ave., University of Michigan, Ann Arbor, MI, USA 48109
[2] Department of Integrative Ecology, Estación Biológica de Doñana, EBD-CSIC, Avda. Américo Vespucio s/n, E-41092 Seville, Spain
[3] Corresponding author; email: jbemmels@umich.edu

Journal:

Molecular Ecology

Contents:

SUPPLEMENTAL METHODS

Generation of ecological niche models

Ecological niche models (ENMs) were used to generate habitat suitability maps for canyon live oak in the present and during the Last Glacial Maximum (LGM, 21.5 ka), using maximum entropy modelling with *Maxent v.3.3.3k* (Phillips *et al.* 2004, 2006) in the *R* package *dismo 1.0-12* (Hijmans *et al.* 2015b).

Species occurrence records were assembled using methods described by Ortego *et al.* (2015). Records were obtained from herbarium databases (Consortium of California Herbaria, *http://ucjeps.berkeley.edu/consortium*; Consortium of Pacific Northwest Herbaria, *http://www.pnwherbaria.org*; University of Arizona Herbarium, *http://ag.arizona.edu/herbarium*; Global Biodiversity Information Facility, *http://www.gbif.org*), as well as our own sampling localities. Only occurrence records from Oregon, California, and Baja California were used to construct ENMs, as our focus was on this portion of the species range. Relict, disjunct populations from Arizona, New Mexico, and Chihuahua might not have been connected with California populations since the LGM and could be adapted to different climatic conditions. Including these populations would potentially bias ENMs intended to predict habitat suitability for California populations. Occurrence records were filtered to remove duplicate records, records with coordinate precision greater than 1 km, records that were within 1 km of another record, and duplicate records that fell within the same grid cell of our climatic data. A total of 1,406 unique observations were retained and used to construct ENMs.

Climatic and topographic data were obtained for both current and LGM conditions. All climate data for LGM conditions were derived from the Community Climate System Model v.4 (CCSM4; Gent *et al.* 2011), which has been shown to perform well for predicting reconstructed terrestrial climate conditions during the LGM (Harrison *et al.* 2014). Thirty-seven climate and topography variables were obtained from which to construct ENMs according to different hypotheses about the determinants of canyon live oak's geographic range (Table S1). Nineteen bioclimatic variables representing temperature and precipitation regimes were obtained directly from the WorldClim Global Climate Dataset (www.worldclim.org; Hijmans *et al.* 2005). We calculated 17 additional variables of interest ourselves that could be derived from the WorldClim variables (Hijmans *et al.* 2005) combined with elevation (also used as a variable by itself; Amante & Eakins 2009) and solar radiation (www.cgiar-csi.org; Zomer *et al.* 2006, 2008). The calculation of these variables is summarized by Title & Bemmels (in prep) from formulae originally described elsewhere (Thornthwaite 1948; Daget 1977; Wang *et al.* 2006, 2012; Zomer *et al.* 2006, 2008; Wilson *et al.* 2007; Sayre *et al.* 2009; Metzger *et al.* 2013; Hijmans *et al.* 2015a). We also estimated annual actual evapotranspiration (AET) using a bucket model (D. Golicher, ECOSUR, San Cristóbal, Mexico; Golicher 2012). AET represents the combination of plant transpiration and evaporation but is difficult to directly measure or estimate because it is impacted by numerous factors (e.g., plant physiology, soil moisture, energy balance, watershed hydrology) operating at different spatial and temporal scales (Zhao *et al.* 2013). The bucket-model method of calculating AET is applicable only for averaging over long time periods at regional scales where local-scale factors such as watershed runoff caused by daily variation in rainfall are less relevant (Golicher 2012).

ENMs were constructed using *Maxent 3.3.3k* (Phillips *et al.* 2004, 2006) with the *R* package *dismo 1.0-12* (Hijmans *et al.* 2015b) at 2.5-arcminute resolution, and were afterwards downscaled to 5-arcminute resolution (approximately 9 by 9 km) to decrease the number of grid cells and improve computational speed of demographic simulations. Habitat-suitability maps were generated for each model for current and LGM conditions. Glaciated regions of the Sierra Nevada and other mountain ranges (Gillespie *et al.* 2004) were masked in LGM habitat-suitability maps by converting habitat-suitability values of these regions to zero.

Selection of environmental variables included in each ENM

The specific environmental variables used to construct the ecological niche models (Table S1) were selected in order to best reflect the ecological factors invoked in each hypothesis, summarized as follows:

(1) *GeneralENM:* as this model tested the impact of response to basic climate variables in a generic ENM, we used all 19 WorldClim bioclimatic variables (Hijmans *et al.* 2005). These variables are frequently used in ecological niche modelling, and represent basic characterizations of overall climate in terms of temperature and precipitation.

(2) *Microsite*: because this model tested the effect of topographic microsite availability, we deliberately did not include any climatic variables. In particular, we hypothesized that areas of high topographic complexity may be most likely to contain ideal microsites for canyon live oak. We therefore included terrain roughness index and slope as measures of topographic complexity. We included elevation and aspect as additional descriptors of topography.

(3) *Multidimension*: because this model tested whether considering multiple aspects of ecological niche is necessary to understand response to climate change, we included all available variables (except elevation; see *Materials and Methods*). The 19 WorldClim bioclimatic variables (Hijmans *et al.* 2005) we included reflect basic climate; the topographic variables consider the impact of microsite availability; and we hypothesized that some of the additional climatic variables we included (Title and Bemmels *in prep*) may characterize climate in a manner more directly physiologically meaningful to determining habitat suitability for a plant. These additional variables included measures of actual and potential evapotranspiration, heat and moisture indices, length of the growing season, and annual heat accumulation (i.e., growing degree-days).

(4) *GrowCold:* for our two trade-off hypotheses, we selected variables that we hypothesized were most relevant to the physiological factors governing the trade-off (in terms of abiotic stress levels, and potential for avoiding or tolerating stress by growing during less stressful periods of the year). Rather than choosing every environmental variable that could in some way potentially be linked to each trade-off, we only selected a few that we assumed were most directly related to the trade-off in particular. We also chose quarterly rather than monthly estimates (when both estimates were available), because quarterly estimates may be better descriptors of overall seasonal climate patterns exerting a general influence on plant physiology and phenology than extremes restricted to a single month.

To construct a model characterizing the potential trade-off between growth rate and cold tolerance, we first chose several temperature variables: mean annual

temperature and Sayre's *et al.* thermicity index as descriptors of overall temperatures; mean temperature of the coldest quarter, which is likely related to the timing and severity of potentially damaging spring and fall frosts when risk of cold injury is highest (Howe *et al.* 2003); and mean temperature of the warmest quarter, which could reflect whether ideal temperatures for growth exist during the summer instead, when cold injury is not a concern. We also chose length of the frost-free period and growing degree-days ≥0ºC and ≥5ºC because these variables describe length of the growing season and available heat accumulation for growth. Conceptually, these variables are likely to reflect respectively the amount of cold stress and overall growth potential experienced by the plant. Finally, we also chose potential evapotranspiration as an additional descriptor of growth potential given unlimited water supply (since precipitation was not hypothesized to be a limiting factor for determining habitat suitability in this model).

(5) *GrowDrought*: To reflect the potential trade-off between growth rate and drought tolerance (note that drought stress primarily occurs during the summer in the California Floristic Province) we chose several variables related to overall and seasonal precipitation: mean annual precipitation and precipitation of the driest and warmest quarters. We further used Thornthwaite's aridity, humidity, and moisture indices, as well as the UNEP aridity index, to characterize overall climatic dryness and moisture availability, and thus the amount of drought stress likely experienced by a plant. Actual evapotranspiration was chosen as a measure of overall growth potential of the plant, given constraints to water supply. Finally, Emberger's pluviothermic quotient, *Q*, was also included, which was originally developed as an index for differentiating among Mediterranean vegetation zones based on a physiologically inspired characterization of annual climatic dryness (Daget 1977). *Q* may thus reflect a continuum between areas of high growth potential and areas of high drought stress.

(6) *LocalAdaptation*: This model tested whether different factors have different relative importance for determining habitat suitability in different ecoregions, within which populations may be locally adapted (see *Materials and Methods*). Because we did not hypothesize a priori which factors would be most important in each specific ecoregion, we included all available variables (except elevation), as in the *Multidimension* hypothesis.

SUPPLEMENTAL TABLES

Table S1. Climatic and topographic variables included when constructing ecological niche models (ENMs) for each iDDC model. An X in the table indicates that a given variable was included in an ENM, and variables with ≥ 5% permutation importance in the *Maxent* ENM algorithm are indicated with an asterisk (*), or with a numerical superscript ($^{1\text{-}6}$) indicating the number of population models for which permutation importance was ≥ 5% for the *LocalAdaptation* model. Citations for variables sources and calculations are as follows: A: Hijmans *et al.* (2005); B: Golicher (2012); C: Title and Bemmels (in prep); D: Zomer *et al.* (2006, 2008); E: Metzger *et al.* (2013); F: Thornthwaite (1948); G: Sayre *et al.* (2009); H: Daget (1977); I: Wang *et al.* (2006, 2012); J: Amante & Eakins (2009); K: Hijmans *et al.* (2015a); L: Wilson *et al.* (2007).

		Model					
Variable	**Citation**	*General-ENM*	*Micro-site*	*Multi-dimension*	*Grow Cold*	*Grow Drought*	*Local Adaptation*
Climate variables							
Bio1 - mean annual temp	A	X		X	X		X
Bio2 - mean diurnal temp range	A	X		X			X
Bio3 - isothermality	A	X		X			X[1]
Bio4 - temp seasonality	A	X*		X*			X[2]
Bio5 - max temp of warmest month	A	X		X			X
Bio6 - min temp of coldest month	A	X		X			X
Bio7 - temp annual range	A	X		X			X
Bio8 - mean temp of wettest quarter	A	X		X			X
Bio9 - mean temp of driest quarter	A	X		X			X
Bio10 - mean temp of warmest quarter	A	X		X	X		X
Bio11 - mean temp of coldest quarter	A	X		X	X*		X
Bio12 - annual precip	A	X		X		X	X
Bio13 - precip of wettest month	A	X		X			X
Bio14 - precip of driest month	A	X*		X*			X[4]
Bio15 - precip seasonality	A	X*		X*			X[4]
Bio16 - precip of wettest quarter	A	X		X			X
Bio17 - precip of driest quarter	A	X		X		X*	X[1]
Bio18 - precip of warmest quarter	A	X		X		X	X
Bio19 - pecip of coldest quarter	A	X*		X			X
actual evapotranspiration (AET)	B			X		X	X[2]
potential evapotranspiration (PET)	C, D			X	X*		X
PET seasonality	C, E			X			X[1]
Thornthwaite's aridity index	C, E, F			X		X	X
Thornthwaite's humidity index	C, E, F			X		X	X[1]
Thornthwaite's moisture index	C, F			X		X	X
UNEP aridity index	C, E			X		X	X[1]
Sayre's et al. thermicity index	C, E, G			X	X		X[1]
Emberger's pluviothermic quotient	C, E, H			X		X*	X[1]
length of frost-free period	I			X	X		X
annual number of frost-free days	I			X			X
growing degree days ≥ 0ºC	C, E			X	X*		X
growing degree days ≥ 5ºC	C, E			X	X*		X
monthCount10deg	C, E			X			X
Topographic variables							
elevation	J		X*				
aspect	C, K		X	X			X
slope	C, K		X	X			X
terrain roughness index (TRI)	C, K, L		X*	X*			X[2]

Table S2. Population and locality geographic coordinates and sample sizes for microsatellite genotyping.

Pop #	Population name	Locality name	Latitude	Longitude	*n*
1	Peninsular Ranges	Laguna Mountain	32.84524	-116.43885	12
1	Peninsular Ranges	Laguna Mountain	32.84954	-116.48535	10
1	Peninsular Ranges	Palomar Mountains	33.28688	-116.80194	2
1	Peninsular Ranges	Palomar Mountains	33.293433	-116.890233	7
1	Peninsular Ranges	Palomar Mountains	33.30272	-116.87217	2
1	Peninsular Ranges	Palomar Mountains	33.30433	-116.87156	4
1	Peninsular Ranges	Palomar Mountains	33.30513	-116.87831	5
1	Peninsular Ranges	Palomar Mountains	33.30585	-116.87193	2
1	Peninsular Ranges	Palomar Mountains	33.31366	-116.87095	2
1	Peninsular Ranges	San Jacinto Mountains	33.68201	-116.68956	3
1	Peninsular Ranges	San Jacinto Mountains	33.6855	-116.69991	1
1	Peninsular Ranges	San Jacinto Mountains	33.68962	-116.70644	2
1	Peninsular Ranges	San Jacinto Mountains	33.69373	-116.71179	4
1	Peninsular Ranges	San Jacinto Mountains	33.7283	-116.72005	4
1	Peninsular Ranges	San Jacinto Mountains	33.74875	-116.73753	1
1	Peninsular Ranges	San Jacinto Mountains	33.79186	-116.74465	2
2	Transverse Ranges	San Bernardino Mountains	34.10532	-116.97227	3
2	Transverse Ranges	San Bernardino Mountains	34.10846	-116.97408	3
2	Transverse Ranges	San Bernardino Mountains	34.11334	-116.97994	4
2	Transverse Ranges	San Bernardino Mountains	34.11794	-116.97784	3
2	Transverse Ranges	San Bernardino Mountains	34.13028	-116.9825	2
2	Transverse Ranges	San Bernardino Mountains	34.16885	-116.89307	3
2	Transverse Ranges	San Gabriel Mountains	34.17832	-117.67668	1
2	Transverse Ranges	San Gabriel Mountains	34.19299	-117.67851	1
2	Transverse Ranges	San Gabriel Mountains	34.35678	-117.74315	4
2	Transverse Ranges	San Gabriel Mountains	34.37137	-117.75443	5
2	Transverse Ranges	San Gabriel Mountains	34.37299	-117.75391	4
2	Transverse Ranges	San Gabriel Mountains	34.2985	-118.14864	2
2	Transverse Ranges	San Gabriel Mountains	34.31516	-118.1368	2
2	Transverse Ranges	San Gabriel Mountains	34.25204	-118.19614	2
2	Transverse Ranges	Los Padres National Forest	34.67807	-119.36795	8
2	Transverse Ranges	Figueroa Mountain	34.72447	-119.95008	9
3	Southern Coast Ranges	Hastings	36.35896	-121.551	11
3	Southern Coast Ranges	Almaden Quicksilver County Park	37.175667	-121.864365	2
3	Southern Coast Ranges	Lick Observatory	37.342607	-121.639584	11
3	Southern Coast Ranges	Mt Diablo State Park	37.88094	-121.92024	4
3	Southern Coast Ranges	Mt Diablo State Park	37.881764	-121.915026	4

3	Southern Coast Ranges	Talmapais State Park	37.904302	-122.604107	1
4	Northern Coast Ranges and Klamath Mountains	Sonoma	38.67822	-123.13693	8
4	Northern Coast Ranges and Klamath Mountains	Willits	39.38811	-123.42426	4
4	Northern Coast Ranges and Klamath Mountains	Willits	39.44133	-123.31432	4
4	Northern Coast Ranges and Klamath Mountains	Redwood Highway	39.92774	-123.75834	5
4	Northern Coast Ranges and Klamath Mountains	Avenue of the Giants	40.21926	-123.81198	2
4	Northern Coast Ranges and Klamath Mountains	Shasta-Trinity National Forest-36 Road	40.38203	-123.29874	5
4	Northern Coast Ranges and Klamath Mountains	Shasta-Trinity National Forest-36 Road	40.41838	-123.45644	1
4	Northern Coast Ranges and Klamath Mountains	Redding	40.60477	-122.5023	12
5	Southern Sierra Nevada	Sequoia National Forest	36.16261	-118.70589	1
5	Southern Sierra Nevada	Sequoia National Park	36.74134	-119.0313	4
5	Southern Sierra Nevada	Sequoia National Park	36.74482	-119.06886	4
5	Southern Sierra Nevada	Stanislaus National Forest - Yosemite National Park	37.66518	-119.80762	2
5	Southern Sierra Nevada	Stanislaus National Forest - Yosemite National Park	37.71377	-119.72743	2
5	Southern Sierra Nevada	Stanislaus National Forest - Yosemite National Park	37.715669	-119.677205	4
5	Southern Sierra Nevada	Stanislaus National Forest - Yosemite National Park	37.731082	-119.604807	1
5	Southern Sierra Nevada	Stanislaus National Forest - Yosemite National Park	37.8161	-119.94467	5
6	Northern Sierra Nevada	Tahoe National Forest	39.28197	-120.98866	10

Table S3. Genetic summary statistics from empirical microsatellite data. Numerical subscripts on summary statistic names refer to population numbers (Fig. 1; Table S2). Mean values are the mean of the individual population values, while total values are calculated over all populations combined. Asterisk (*): number of alleles (*K*) was not included as a summary statistic for model selection (see *Materials and Methods* for explanation).

Summary statistic	Observed value
Heterozygosity	
H_1	0.7506
H_2	0.7541
H_3	0.7761
H_4	0.7546
H_5	0.7662
H_6	0.6893
H_{mean}	0.7485
H_{total}	0.7779
Population differentiation	
F_{ST}	0.0330
$F_{ST(2,1)}$	0.0077
$F_{ST(3,1)}$	0.0356
$F_{ST(3,2)}$	0.0326
$F_{ST(4,1)}$	0.0434
$F_{ST(4,2)}$	0.0420
$F_{ST(4,3)}$	0.0094
$F_{ST(5,1)}$	0.0312
$F_{ST(5,2)}$	0.0264
$F_{ST(5,3)}$	0.0204
$F_{ST(5,4)}$	0.0310
$F_{ST(6,1)}$	0.0713
$F_{ST(6,2)}$	0.0814
$F_{ST(6,3)}$	0.0817
$F_{ST(6,4)}$	0.0635
$F_{ST(6,5)}$	0.0595
*Number of alleles**	
K_1	13.23
K_2	13.31
K_3	12.15
K_4	10.92
K_5	10.15
K_6	5.08
K_{mean}	10.81
K_{total}	17.85

Table S4. Ability of each model to generate simulated summary statistics in agreement with summary statistics of the empirical data. A simulated distribution of summary-statistic values was generated for each model (10^5 simulations per model; parameter values drawn from prior distribution), and the percentile corresponding to the empirical summary-statistic value within this distribution was calculated. Reported in the table is the distance between the empirical value and the median (50^{th} percentile) of the simulated distribution (possible values: -50 to +50); values approaching ± 50 indicate summary statistics that are difficult to fit, whereas values close to zero indicate that simulated values were similar to those observed in the empirical data. For example, a value of (+) 9.7 indicates that the empirical value is 9.7 percentiles above the simulated median value (i.e., the 59.7^{th} percentile overall). Shading has been added to cells for visual clarity: no shading, empirical value within ± 20 percentiles of the simulated median value; light grey, within ± 20-30 percentiles; dark grey, ± 30-40 percentiles; black, ± 40-50 percentiles. Asterisk (*): number of alleles (*K*) was not included as a summary statistic for model selection (see *Materials and Methods* for explanation).

	Model					
Summary statistic	***General-ENM***	***Microsite***	***Multi-dimension***	***GrowCold***	***Grow-Drought***	***Local-Adaptation***
Heterozygosity						
H_1	(+) 9.7	(+) 6.3	(+) 11.4	(+) 10.1	(+) 10.5	(+) 9.2
H_2	(+) 12.9	(+) 8.5	(+) 10.7	(+) 14.9	(+) 10.7	(+) 22.8
H_3	(+) 19.6	(+) 27.3	(+) 35.3	(+) 41.5	(+) 17.1	(+) 25.9
H_4	(+) 9.4	(+) 7.3	(+) 30.7	(+) 27.6	(+) 8.4	(+) 7.7
H_5	(+) 9.4	(+) 9.0	(+) 8.7	(+) 8.7	(+) 8.8	(+) 23.8
H_6	(+) 3.5	(+) 0.7	(+) 3.6	(+) 5.3	(+) 2.0	(+) 4.4
H_{mean}	(+) 10.7	(+) 9.7	(+) 19.9	(+) 21.8	(+) 9.4	(+) 16.2
H_{total}	(+) 9.0	(+) 7.8	(+) 8.1	(+) 10.1	(+) 8.4	(+) 9.3
Population differentiation						
$F_{ST(2,1)}$	(-) 43.1	(-) 28.1	(-) 45.0	(-) 43.0	(-) 43.9	(-) 45.9
$F_{ST(3,1)}$	(-) 14.9	(-) 19.4	(-) 39.6	(-) 43.0	(-) 21.2	(-) 26.7
$F_{ST(3,2)}$	(-) 21.2	(-) 23.8	(-) 39.2	(-) 43.6	(-) 14.9	(-) 39.7
$F_{ST(4,1)}$	(+) 7.4	(+) 29.9	(-) 38.8	(-) 33.7	(-) 1.0	(+) 8.6
$F_{ST(4,2)}$	(-) 2.0	(+) 19.1	(-) 38.5	(-) 35.7	(+) 5.3	(-) 28.8
$F_{ST(4,3)}$	(-) 34.2	(-) 39.6	(-) 45.1	(-) 45.3	(-) 33.0	(-) 39.0
$F_{ST(5,1)}$	(-) 0.3	(+) 18.2	(-) 18.6	(+) 5.1	(-) 12.6	(-) 35.7
$F_{ST(5,2)}$	(-) 15.3	(+) 2.6	(-) 14.8	(-) 14.0	(-) 7.9	(-) 42.9
$F_{ST(5,3)}$	(-) 19.3	(-) 32.0	(-) 42.1	(-) 44.7	(-) 16.7	(-) 42.7
$F_{ST(5,4)}$	(+) 8.9	(+) 12.8	(-) 41.6	(-) 37.2	(+) 11.4	(-) 34.0
$F_{ST(6,1)}$	(+) 25.8	(+) 44.7	(+) 6.9	(+) 17.8	(+) 27.4	(+) 12.4
$F_{ST(6,2)}$	(+) 23.3	(+) 41.4	(+) 18.6	(+) 19.4	(+) 33.2	(-) 13.5
$F_{ST(6,3)}$	(+) 17.9	(+) 5.5	(-) 22.7	(-) 33.5	(+) 25.1	(-) 5.8
$F_{ST(6,4)}$	(+) 25.1	(+) 39.3	(-) 30.3	(-) 25.5	(+) 33.5	(+) 17.3
$F_{ST(6,5)}$	(+) 27.8	(+) 37.3	(+) 17.9	(+) 25.3	(+) 36.2	(-) 23.4
F_{ST}	(-) 12.6	(+) 5.6	(-) 36.9	(-) 35.5	(-) 9.4	(-) 38.4
*Number of alleles**						
K_1	(+) 28.4	(+) 26.8	(+) 29.8	(+) 26.8	(+) 27.8	(+) 27.3
K_2	(+) 30.3	(+) 27.7	(+) 28.8	(+) 30.5	(+) 28.3	(+) 34.5
K_3	(+) 45.3	(+) 47.5	(+) 49.1	(+) 49.9	(+) 44.4	(+) 47.1
K_4	(+) 26.4	(+) 25.6	(+) 43.4	(+) 40.5	(+) 24.8	(+) 24.8
K_5	(+) 21.5	(+) 21.6	(+) 20.9	(+) 20.6	(+) 20.2	(+) 30.0
K_6	(+) 1.5	(-) 0.4	(+) 1.0	(+) 1.6	(+) 0.6	(+) 0.8
K_{mean}	(+) 25.6	(+) 24.9	(+) 28.8	(+) 28.0	(+) 24.0	(+) 27.4
K_{total}	(+) 28.5	(+) 28.2	(+) 28.0	(+) 28.7	(+) 27.5	(+) 28.2

SUPPLEMENTAL FIGURES

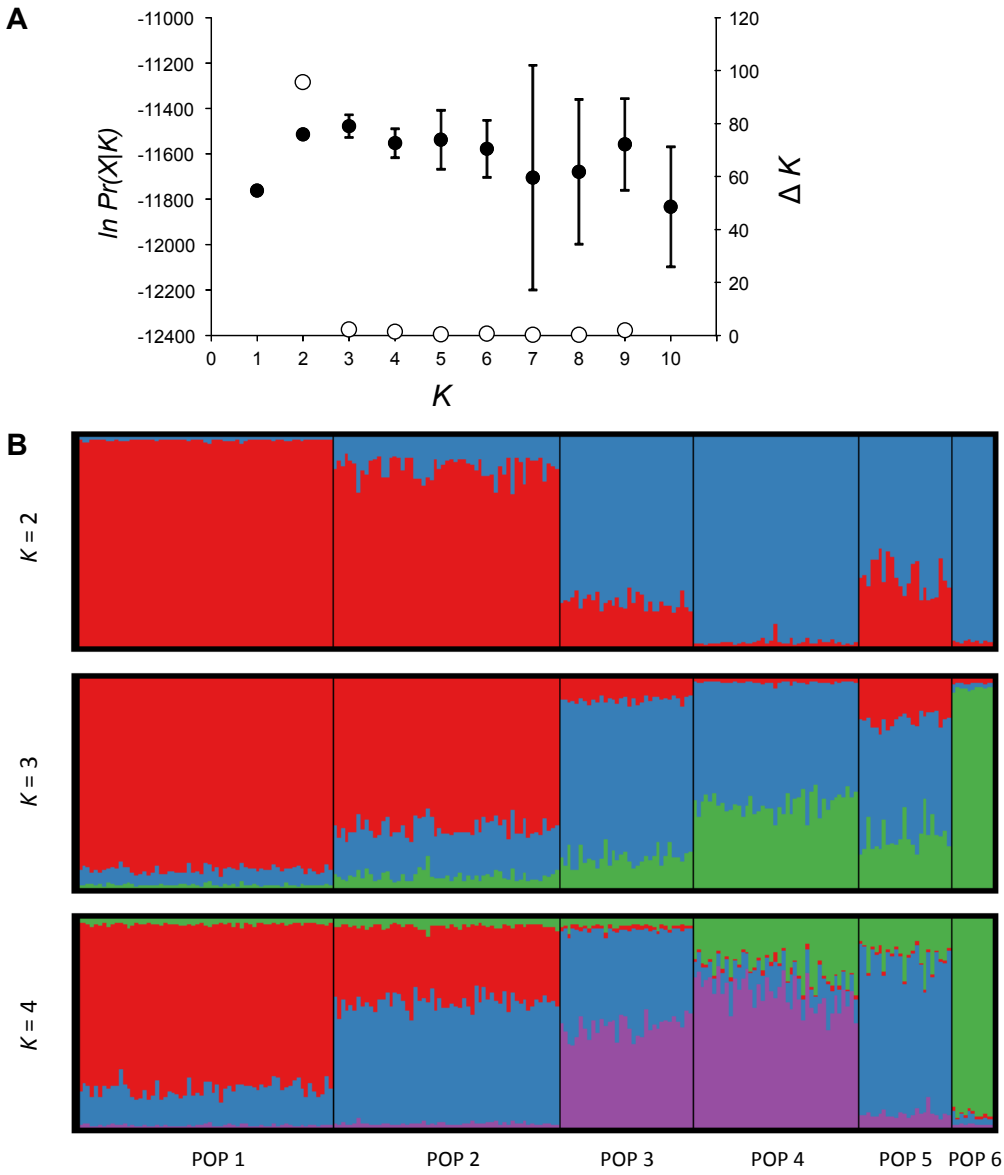

Figure S1. Results of Bayesian clustering analyses in *STRUCTURE*. (a) Plots show the mean (± SD) log probability of the data (*ln Pr(X|K)*) over 10 runs (left axis, black dots and error bars) and the magnitude of Δ*K* (right axis, open dots) for each value of *K* (number of clusters). (b) Genetic assignments of individuals based on the Bayesian analyses implemented in the program *STRUCTURE*. Each individual is represented by a vertical bar, which is partitioned into *K* coloured segments showing the individual's probability of belonging to the cluster with that colour. Thin vertical black lines separate individuals from the main geographical regions considered in this study according to population (see Fig. 1). Populations are defined as follows: (1) Peninsular Ranges, (2) Transverse Ranges, (3) Southern Coast Ranges, (4) Northern Coast Ranges and Klamath Mountains, (5) Southern Sierra Nevada, and (6) Northern Sierra Nevada.

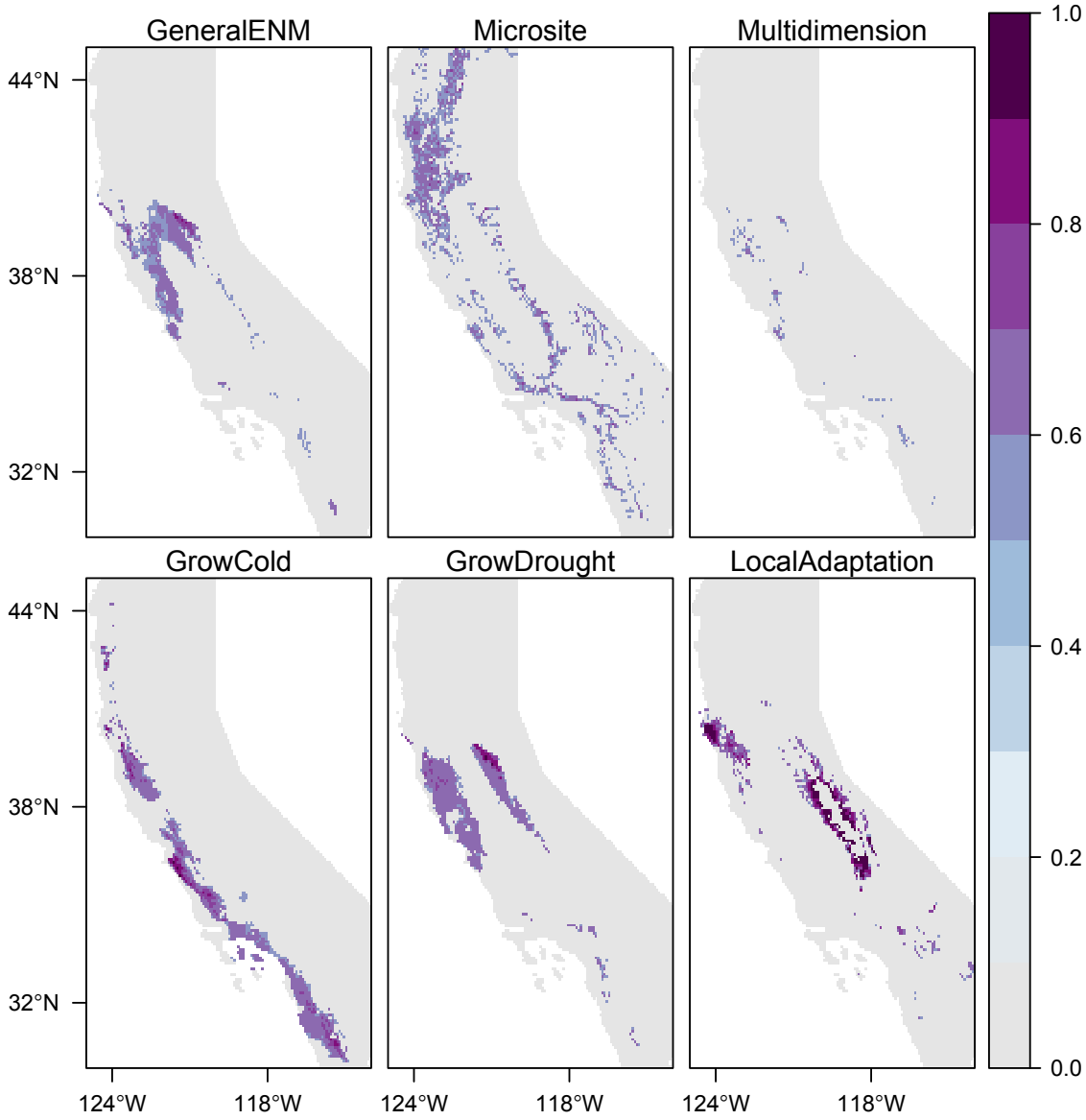

Figure S2. Habitat suitability in ancestral source populations of canyon live oak from which demographic simulations were initiated for each model.

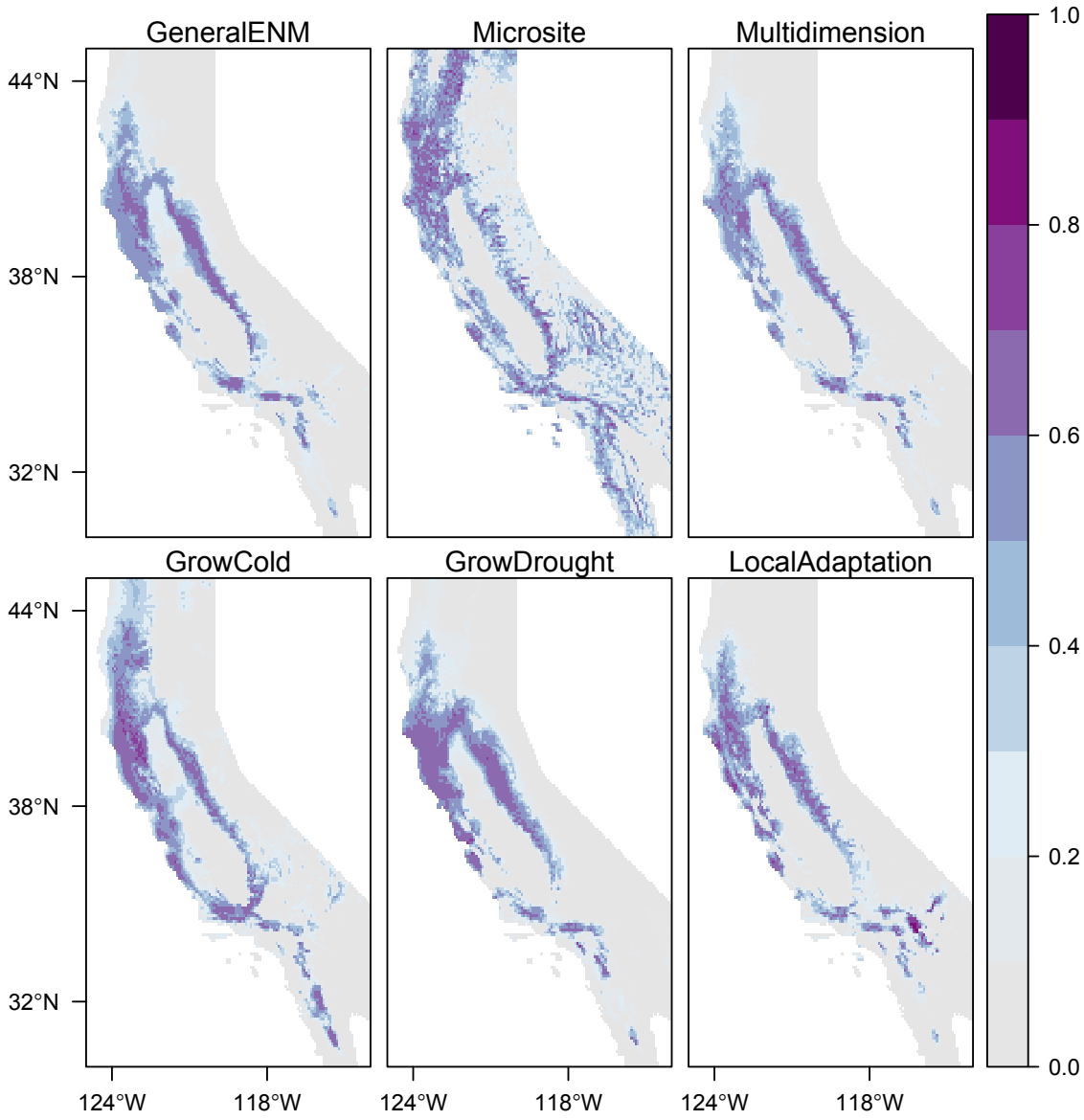

Figure S3. Current habitat suitability for canyon live oak from ecological niche models constructed for each iDDC model.

LITERATURE CITED

Amante C, Eakins BW (2009) ETOPO1 1 arc-minute global relief model: procedures, data sources and analysis. NOAA Technical Memorandum NESDIS NGDC-24. *National Geophysical Data Center, NOAA*.

Daget P (1977) Le bioclimat méditerranéen: analyse des formes climatiques par le système d'Emberger. *Vegetatio*, **34**, 87–103.

Gent PR, Danabasoglu G, Donner LJ *et al.* (2011) The Community Climate System Model version 4. *Journal of Climate*, **24**, 4973–4991.

Gillespie A, Porter S, Atwater BF (2004) *Quaternary glaciations - extent and chronology. Part II: North America. Additional CD-ROM*. Elsevier, San Diego, CA.

Golicher D (2012) Implementing a bucket model using WorldClim layers. https://rpubs.com/dgolicher/2964. *RPubs*.

Harrison SP, Bartlein PJ, Brewer S *et al.* (2014) Climate model benchmarking with glacial and mid-Holocene climates. *Climate Dynamics*, **43**, 671–688.

Hijmans RJ, Cameron SE, Parra JL, Jones PG, Jarvis A (2005) Very high resolution interpolated climate surfaces for global land areas. *International Journal of Climatology*, **25**, 1965–1978.

Hijmans RJ, van Etten J, Cheng J *et al.* (2015a) Package "raster". https://cran.r-project.org/web/packages/raster/index.html.

Hijmans RJ, Phillips S, Leathwick J, Elith J (2015b) Package "dismo". http://cran.r-project.org/web/packages/dismo/index.html.

Howe GT, Aitken SN, Neale DB *et al.* (2003) From genotype to phenotype: unraveling the complexities of cold adaptation in forest trees. *Canadian Journal of Botany*, **81**, 1247–1266.

Metzger MJ, Bunce RGH, Jongman RHG *et al.* (2013) A high-resolution bioclimate map of the world: A unifying framework for global biodiversity research and monitoring. *Global Ecology and Biogeography*, **22**, 630–638.

Ortego J, Gugger PF, Sork VL (2015) Climatically stable landscapes predict patterns of genetic structure and admixture in the Californian canyon live oak. *Journal of Biogeography*, **42**, 328–338.

Phillips SJ, Anderson RP, Schapire RE (2006) Maximum entropy modeling of species geographic distributions. *Ecological Modelling*, **190**, 231–259.

Phillips SJ, Dudík M, Schapire RE (2004) A maximum entropy approach to species distribution modeling. *Proceedings of the Twenty-First International Conference on Machine Learning*, 655–662.

Sayre R, Comer P, Warner H, Cress J (2009) *A new map of standardized terrestrial ecosystems of the conterminous United States: US Geological Survey Professional Paper 1768*. Reston, VA.

Thornthwaite CW (1948) An approach toward a rational classification of climate. *Geographical Review*, **38**, 55–94.

Title PO, Bemmels JB (in prep) ENVIREM: an expanded set of bioclimatic variables improves ecological niche modeling performance. *Methods in Ecology and Evolution*.

Wang T, Hamann A, Spittlehouse DL, Aitken SN (2006) Development of scale-free climate data for western Canada for use in resource management. *International*

Journal of Climatology, **26**, 383–397.
Wang T, Hamann A, Spittlehouse DL, Murdock TQ (2012) ClimateWNA—high-resolution spatial climate data for western North America. *Journal of Applied Meteorology and Climatology*, **51**, 16–29.
Wilson MFJ, O'Connell B, Brown C, Guinan JC, Grehan AJ (2007) Multiscale terrain analysis of multibeam bathymetry data for habitat mapping on the continental slope. *Marine Geodesy*, **30**, 3–35.
Zhao L, Xia J, Xu C-Y *et al.* (2013) Evapotranspiration estimation methods in hydrological models. *Journal of Geographical Sciences*, **23**, 359–369.
Zomer RJ, Trabucco A, Bossio DA, Verchot L V. (2008) Climate change mitigation: A spatial analysis of global land suitability for clean development mechanism afforestation and reforestation. *Agriculture, Ecosystems & Environment*, **126**, 67–80.
Zomer RJ, Trabucco A, Van Straaten O, Bossio DA (2006) *Carbon, Land and Water: A Global Analysis of the Hydrologic Dimensions of Climate Change Mitigation through Afforestation/Reforestation. International Water Management Institute Research Report 101.* Colombo, Sri Lanka.